

Influence of Organophilic Clay and Preparation Methods on EVA/Montmorillonite Nanocomposites

Yong Tang,¹ Yuan Hu,¹ Junzhong Wang,^{1,2} Ruowen Zong,¹ Zhou Gui,¹ Zuyao Chen,² Yonglong Zhuang,³ Weicheng Fan¹

¹State Key Lab of Fire Science, Anhui University, Hefei, 230026, Anhui, China

²Department of Chemistry, University of Science and Technology of China, Anhui University, Hefei, 230026, Anhui, China

³Analyses and Test Center, Anhui University, Hefei, 230026, Anhui, China

Received 16 January 2003; accepted 23 April 2003

ABSTRACT: Ethylene-vinyl acetate copolymer (EVA)/montmorillonite MMT nanocomposites have been prepared by using different methods: one is from the organophilic montmorillonite (OMT) and the other is from the pristine MMT and reactive compatibilizer hexadecyl trimethyl ammonium bromide (C16). In this study, different kneaders were used (twin-screw extruder and twin-roll mill) to prepare nanocomposites. The nanocomposite structures are evidenced by the X-ray diffraction (XRD) and high-resolution electronic microscope (HREM). The thermal properties of

the nanocomposites were investigated by thermogravimetric analysis (TGA). Moreover, the tensile tests were carried out with a Universal testing machine DCS-5000. It is shown that different methods and organophilic montmorillonite have influence on EVA/MMT nanocomposites. © 2003 Wiley Periodicals, Inc. *J Appl Polym Sci* 91: 2416–2421, 2004

Key words: matrix; organoclay; MMT; nanocomposites; intercalated

INTRODUCTION

Nanocomposites are particle-filled polymers for which at least one dimension of the dispersed particles is in the nanometer range. Polymer layered silicate nanocomposites (PLSNs), which are hybrids, are composed layered silicates dispersed in a polymer matrix in the form of reticular layers of crystals about 1 nm thick and with a lamellar aspect ratio of between 100 and 1000. The molecular level interaction created in the PLSN is likely to affect not only physical properties, but also its chemical behaviors.¹

Ethylene-vinyl acetate copolymer (EVA) is a copolymer used for many applications, including the electrical cable sheathing industry. An important objective pursued by manufacturers is to produce a flame-retardant polymer, without affecting the mechanical properties of the material. In this article, different organophilic montmorillonites (OMT) have been used to prepare EVA/montmorillonite (MMT) nanocomposites and at the same time a novel method² was used to prepare EVA/MMT nanocomposites by melt

intercalation, by using pristine clay and EVA. By so doing, a cationic surfactant such as an ammonium salt bearing long alkyl chains (hexadecyl trimethyl ammonium bromide, C16) has been used as a polymer/clay reactive compatibilizer. The thermal analysis and the tensile tests were investigated in this work. Moreover, we discuss the probable mechanism of the intercalation.

EXPERIMENTAL

Materials

EVA was supplied as pellets by Beijing Petrochemical (China). The pristine MMT (with a cation exchange capacity of 97 meq/100 g) was kindly provided by Ke Yan Co. (Hefei, China). Octadecylammonium (C18) and C16 were bought from Shanghai Chemistry Co.

The preparation of organophilic clay

Organophilic clay was prepared by cation exchange of nature counterions with amine surfactants according to the method of Kawasumi et al.³ The amines used were C18 and C16, and the organophilic clay was termed OMT1 and OMT2, respectively. In this article, OMT3 was prepared as follows: at first, the C16 was solubilized in alcohol at 30°C; then the wet MMT with alcohol was added into a blender (high-speed mixture machine, 730–1450 rpm); then the blending was milled at high speed for half an hour. In this work, the three

Correspondence to: Y. Hu (yuanhu@ustc.edu.cn).
Contract grant sponsor: National Natural Science Foundation of China; contract grant number: 50003008
Contract grant sponsor: China NKBRFSF Project.
Contract grant sponsor: 2001CB409600.

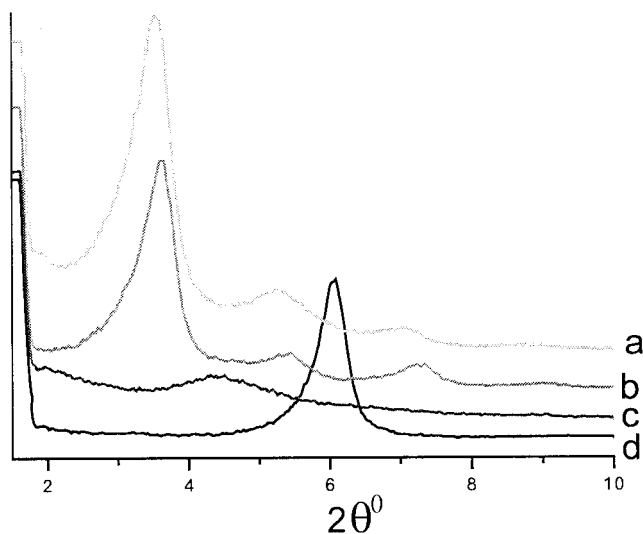


Figure 1 XRD patterns for (a) OMT1; (b) OMT2; (c) OMT3; (d) MMT.

types organophilic clay were dried under vacuum at 100°C for several hours before using. The interlayer spacing for pure and treated MMT was measured by X-ray diffraction (Fig. 1, Table I).

The preparation of eva/mmt nanocomposites

The preparation of EVA/MMT nanocomposites used two different methods. The conventional method⁴ was used. The pellets of EVA and OMT were melt-blended at 145°C for 12 min by using a twin-roll mill (XK-160, 50 r/min, JiangShu, China) or twin-screw extruder (TE-35, $L/D = 48$, 30–600 rpm, JiangShu) to yield the hybrids. The compounding using the twin-screw extruder was carried out at 180–210°C, screw speed of 200 rpm, and a feed rate of 7.74 kg/h. The mean value of the residence time for pure polypropylene (PP) at this condition is about 2.3 min. Another new method was used in this work. First, the pristine MMT (dried powder) and C16 were mixed and ground together in a mortar and pestle; then, the mixed powder (MMT+C16) was added into molten EVA (EVA was added to the mill at the beginning of the blending procedure). Table II shows the mixing weight ratio of the samples.

Evaluation of dispersibility of the clay in PP matrix

The dispersion of the MMT was evaluated by means of X-ray diffractometry (XRD) and high-resolution electronic microscope (HREM). XRD analysis was carried out (Cu , $\lambda = 1.54178 \text{ \AA}$, between $2\theta = 1.5$ and 10°) on the samples and pristine MMT. The HREM specimens of EVA/MMT nanocomposites were cut from an epoxy block with the embedded film at a low temper-

ature by using an ultramicrotome (Ultracut-1, UK) with a diamond knife. Thin specimens of 50–80 nm were collected in a trough filled with a solution of dimethylsulfoxide and glycerin and then placed on 200-mesh copper grids. HREM images were obtained with a JEOL 2010 microscope at an acceleration voltage of 200 kV.

Thermal stability

The samples were analyzed by thermogravimetric analysis (TGA) by using a Netzsch STA-409c thermal analyzer under nitrogen flow from 25 to 600°C at a rate of 10°C/min. The TG curves are shown in Figure 6.

Tensile test

The tensile tests were carried out with a Universal testing machine DCS-5000 (Shimadzu, Japan) at a head speed of 50 mm/min. All measurements were done in five replicates and the value was averaged. The results of the tests are shown in Table IV.

RESULTS AND DISCUSSION

Dispersibility of EVA/MMT hybrids

Figure 1 shows XRD profiles of MMT and treated MMT. The peaks correspond to the (001) reflections of the clay. The d_{001} peak of pristine MMT at $2\theta = 5.8^\circ$ corresponds to 1.4 nm [Fig. 1(d)] interlayer spacing. The d_{001} peaks of treated MMT are observed at a lower angle than that of pristine MMT; these indicate the amines intercalate into the silicate layers and expand the basal spacing. From Figure 1, it can be seen the three types of OMT have different interlayer spacing (Table I). The interlayer spacing of OMT1 [Fig 1(a)] is bigger than that of other two [Fig 1(b, c)]. The diffraction intensity of OMT3 [Fig 1(c)] is very weak. This may be that only a little amine (C16) intercalates into the silicate layers and at the same time this modified method made the crystal lattice deformation or interlayer distance inhomogeneous.

Figure 2 shows the XRD patterns of the EVA/OMT hybrids and three types of OMT. Figure 2(a1) shows that the silicate laminates have lost their reciprocal order compared with the interlayer spacing of OMT1 (2.50 nm). The HREM image of EVA/OMT1 (EVA1) is

TABLE I
The Interlayer Distance of OMMT

Clay	Amine	Interlayer distance (Å)
MMT	—	14.82
OMT1	C18	25.04
OMT2	C16	24.65
OMT3	C16	19.84

TABLE II
The Compositions of the EVA/Clay Hybrids

Sample	Clay (wt %)	Compatibilizer (C16) (wt %)	Kneader	Polymer EVA (wt %)
EVA1	OMT1 (5)		twin-roll mill	EVA (95)
EVA2	OMT2 (5)		twin-roll mill	EVA (95)
EVA3	OMT3 (5)		twin-roll mill	EVA (95)
EVA4	MMT (5)	C16 (2.5)	twin-roll mill	EVA (92.5)
EVA5	OMT2 (5)		twin-screw extruder	EVA (95)

reported in Figure 3(a). Individual silicate layers [marked A in Fig 3(a)] are observed to be well-dispersed (exfoliated) in the polymer matrix. In addition, some large intercalated tactoids [marked B in Fig. 3(a)] are also visible in the image. Figure 2(b1) shows that the (001) plane reflections are observed at a lower angle than that of OMT2, which indicates that EVA intercalates between the layers of OMT2 during melt blending. From Figure 3(b), the intercalated morphology can be seen. As for the EVA/OMT3 hybrid, the XRD shows that the (001) plane reflections have disappeared. This may be that the diffraction of the OMT3 [Fig 1(c)] is very weak; when OMT3 was added into the EVA matrix, the diffraction intensity decreased further compared to that of OMT3. In the HREM image [Fig 3(c)] of EVA/OMT3 (EVA3), the primary particles, composed of many silicate layers, can be seen. There is no intercalation of the polymer between the layers.

Figure 4 shows the XRD patterns of the EVA/OMT hybrids prepared by different methods or different kneaders. The d_{001} peak of the EVA4 [Fig. 4(a)] is observed at a lower angle ($2\theta = 2.3^\circ$) than that of pristine clay ($2\theta = 5.8^\circ$), which indicates the average of

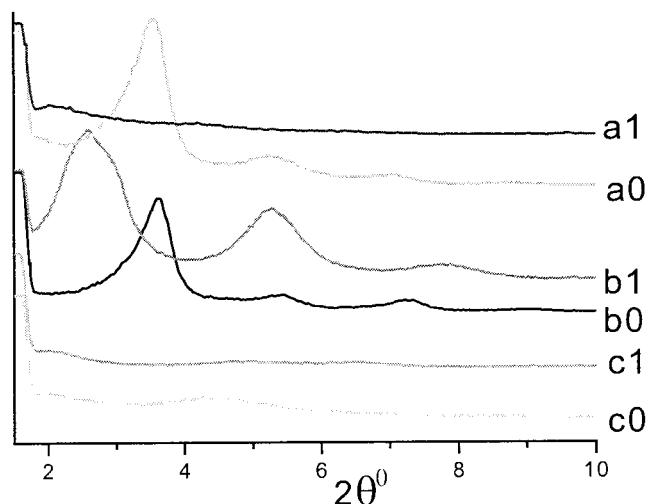
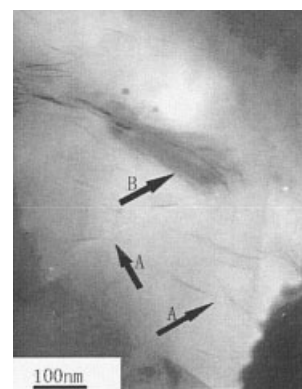


Figure 2 XRD patterns for EVA/clay hybrids (a0) OMT1; (a1) EVA/OMT1; (b0) OMT2; (b1) EVA/OMT2; (c0) OMT3; (c1) EVA/OMT3.



(a)



(b)



(c)

Figure 3 The TEM images of EVA/clay hybrids: (a) EVA1; (b) EVA2; (c) EVA3.

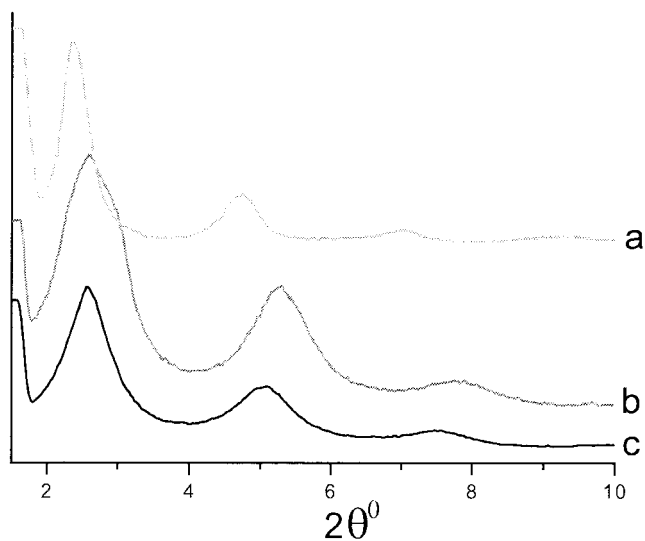
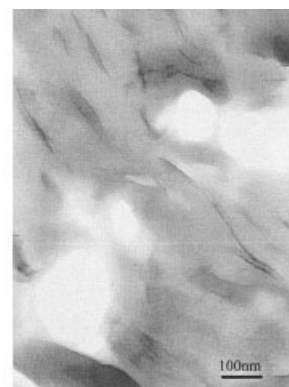


Figure 4 XRD patterns for (a) EVA4; (b) EVA2; (c) EVA5.

basal spacing increase from 1.4 to 3.78 nm. These results indicate the EVA with C16 could intercalate into the silicate layers and expand the basal spacing. The dispersibility of the silicate layers in the EVA is also confirmed by HREM shown in Figure 5(a). The image confirmed that EVA-layered silicate nanocomposites are formed. As for EVA2 and EVA5, XRD shows the difference of the two compounds prepared by different kneaders. It can be seen that the distance of the interlayer of EVA5 (3.46 nm) is bigger than that of EVA2 (3.32 nm). At the same time, the HREM image of EVA5 [Fig. 5(b)] shows that the dispersibility of organophilic MMT in EVA5 is much better than that of OMT in EVA2. The silicates dispersed in a regular manner relative to silicates in EVA2, which may be the high-shear force of the twin-screw extruder.

Thermogravimetry

Thermal stability is an important property for which the nanocomposite morphology plays an important role. EVA polymer and some composites were analyzed by TGA. EVA undergoes two degradation steps,⁵ as shown in Figure 6. The first decomposition step is due to acetic acid and the formation of double bonds occurs between 300 and 400°C with a maximum around 350°C. The second degradation step involves the polymeric chain and leads to the complete polymer volatilization. The 5% loss temperature ($T_{-5\%}$) and the maximum weight-loss temperatures (T_{\max} including two degradation steps, $T_{\max1}$ and $T_{\max2}$, respectively) and char residue at 600°C are listed in Table III. The results for the intercalated or exfoliated EVA/MMT nanocomposites show that the first degradation step takes place without a strong catalytic effect, as reported in the literature.⁵ However, the



(a)



(b)

Figure 5 The TEM images of (a) EVA4; (b) EVA5.

$T_{-5\%}$ temperatures of some nanocomposites are lower than that of pure EVA polymer or EVA/MMT microcomposites. The OMT and kneaders have influence on

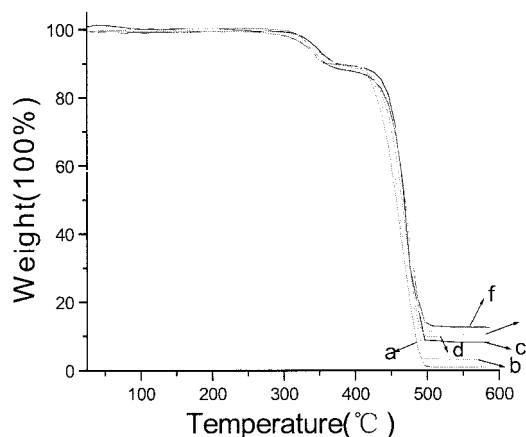


Figure 6 The TG curves for EVA and EVA/clay hybrids (a) pure EVA; (b) EVA3; (c) EVA2; (d) EVA5; (e) EVA1; (f) EVA4.

TABLE III
Thermal Properties of EVA and EVA/Clay Hybrids

Sample	$T_{-5\%}$ (°C)	$T_{\max 1}$ (°C)	$T_{\max 2}$ (°C)	Char residue at 600 °C (wt %) ^a
EVA0	336.5	339.9	466.4	0.86
EVA1	332.3	341.9	474.6	5.16
EVA2	344.3	348.8	471.2	3.32
EVA3	341.9	348.6	463.6	1.7
EVA4	330.9	348.4	473.2	7.14
EVA5	330.2	350.9	477.4	4.84

^a The char for OMT or MMT with C16 at 600°C has already been subtracted.

the $T_{-5\%}$ temperature. EVA1 and EVA2 were melt-blended from OMT1 and OMT2, respectively. The HREM images show that EVA1 have exfoliated and intercalated morphology, but only intercalated morphology can be seen in the images of EVA2. EVA5 was melt-blended by using a twin-screw extruder, so the dispersibility of organophilic MMT in EVA5 is better than that of OMT in EVA2. Table III show that the $T_{-5\%}$ of EVA1 and EVA5 are lower than that of EVA2, which may be that⁶ there is intimate contact between the polymer molecules and the atoms of the inorganic crystalline layers relative to silicates in EVA2. The catalytic effects of acidic sites of the layered silicates deriving from Hoffman elimination reaction⁷ of the organic alkylammonium cation are more effective than that in EVA2. So the onset temperatures of EVA1 and EVA5 are a little lower than that of EVA2. The similar phenomenon was observed in the TG curves of EVA4. As for EVA3, where the silicates are dispersed microscopically, it behaves in the same way as pure EVA. The second degradation step for EVA/MMT nanocomposites display a slight stabilization of about 10°C throughout the process. Figure 6 shows the residue weight increased in the order of EVA4 > EVA1 > EVA5 > EVA2 > EVA3 > EVA0.

Tensile test

Table IV shows the results of the tensile test of the EVA/MMT hybrids. The tensile strength of EVA/MMT nanocomposites is not much improved, com-

TABLE IV
Tensile Properties of EVA and EVA/Clay Hybrids

Sample	Stress at break (Mpa)	Strain at break (%)
EVA0	11.02	402
EVA1	11.15	412
EVA2	11.08	409
EVA3	10.40	347
EVA4	11.09	428
EVA5	11.31	468

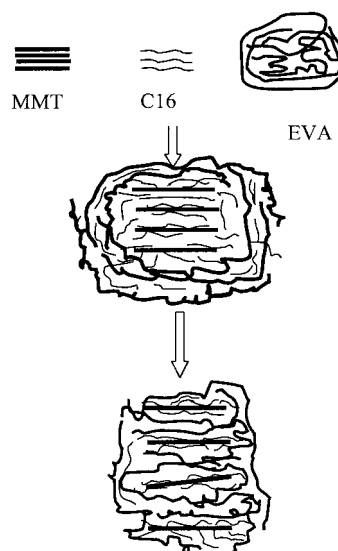


Figure 7 Schematic representation of the intercalation process of EVA with C16 into pristine MMT.

pared with pure EVA. From Table IV, it can be seen that EVA5, produced by twin-screw extruder, shows relatively higher stress at break and strain at break than those observed for the other compounds, which may be that different dispersions of silicates have influence on the mechanical properties. As for EVA3 (microcomposites), the stress at break and strain at break are lower than those of pure EVA.

Discuss the probable mechanism of intercalation

In this work, a novel method was used to prepare EVA/MMT nanocomposites starting from pristine MMT and reactive compatibilizer C16. The probable mechanism may be that this system is a reactive process during melt-mixing. The prominent interaction will arise between the three components⁸ of the system—the silicate surface, the surfactant chains (C16), and the polymer matrix. At first, some surfactant chains diffuse into the interlayer under physical absorption and shear. Because the negative charge originates in the silicate layer, the cationic head group of the surfactant will preferentially reside at the layer surface and the aliphatic tail will radiate away from the surface.⁹ In fact, this course just makes the MMT organophilic, which will reduce the interfacial energies.⁸ However, there is some difference in this system because the surfactant does not diffuse into the interlayer at the same time; that is to say, there is some surfactant stay at the polymer matrix (EVA), which may enhance the compatibility when the polymer matrix intercalated into interlayer. In fact, there is an interaction between the polymer matrix and the surfactant, just like the interaction between the surfactant and the silicates. When the packing density in the

interlayer increases to an appropriate value, intercalation of the polymer matrix molecular chains begins with the help of shear force until forming the exfoliated or intercalated structure. The scheme of this kind of compound is shown in Figure 7.

CONCLUSION

EVA/MMT nanocomposites were prepared by melt intercalation with two methods starting from OMT and pristine MMT by adding a surfactant (C16). The different OMT and methods have influence on the morphology, thermal stability, and mechanical properties of EVA/MMT nanocomposites. The study showed that in these systems samples prepared by one pot have higher thermal stability and samples prepared by using the twin-screw extruder have better mechanical properties. The probable mechanism of intercalation about the novel method was discussed in this work.

The work was financially supported by the National Natural Science Foundation of China (No. 50003008), the China NK-BRSF Project (No. 2001CB409600), and Anhui "the tenth five years" tackle key problems project.

References

1. Alexander, M.; Dubois, P. *Mater Sci Eng* 2000, 1, 28.
2. Alexandre, M.; Beyer, G.; Henrist, C.; Cloots, R.; Jerome, A. R. R.; Dubois, P. *Chem Mater* 2001, 13, 3830.
3. Kawasumi, M.; Hasegawa, N.; Kato, M.; Usuki, A.; Okade, A. *Macromolecules* 1997, 30, 6333.
4. Zanetti, M.; Kashiwagi, T.; Falqui, L.; Camino, G. *Chem Mater* 2002, 14, 881.
5. Zanetti, M.; Camino, G.; Thomann, R.; Mülhaupt, R. *Polymer* 2001, 42, 4501.
6. Tang, Y.; Hu, Y.; Wang, S.-F.; Gui, Z.; Chen, Z.; Fan, W. *Polym Degrad Stab* 2002, 78, 555.
7. Xie, W.; Gao, Z.; Pan, W.-P.; Hunter, D.; Singh, A.; Vaia, R. *Chem Mater* 2001, 13, 2979.
8. Vaia, R. A.; Giannelis, E. P. *Macromolecules* 1997, 30, 7990.
9. Vaia, R. A.; Teukoisky, R. K.; Giannelis, E. P. *Chem Mater* 1994, 6, 1017.